Anisotropic localization behavior of graphene in the presence of diagonal and off-diagonal disorders*

Wang Li-Min(王莉敏)†, Shi Shao-Cong(拾邵聪), and Zhang Wei-Yi(章维益)

The National Laboratory of Solid State Microstructures and the Department of Physics, Nanjing University, Nanjing 210093, *China*

(Received 29 May 2013; revised manuscript received 23 July 2013)

Anisotropic localization of Dirac fermions in graphene along both the x and y axes was studied using the transfer-matrix method. The two-parameter scaled behavior around the Dirac points was observed along the x axis with off-diagonal disorder. In contrast, the electronic state along the y axis with armchair edges was delocalized, which can be described well by single parameter scaling theory. This implies that the breakdown of the single-parameter scaling is related to the zigzag edge along the x axis. Furthermore, dimerization induced by the substrate suppresses the two-parameter scaling behavior along the x axis and preserves the delocalized state along the y axis. Our results also demonstrate anisotropic localization in graphene with diagonal disorder that can be tuned by dimerization.

Keywords: anisotropic localization, graphene, dimerization

PACS: 72.80.Ng, 73.20.Fz, 64.60.F−, 81.05.Vp **DOI:** 10.1088/1674-1056/22/12/127201

1. Introduction

Since graphene was fabricated by Novoselov *et al.*,[1–4] its remarkable properties have been investigated experimentally[5–8] and theoretically.[9–14] Graphene is an important two-dimensional electronic system that is distinct from the typical two-dimensional electron gases hosted in common semiconductor heterostructures. The electrons in graphene can be approximately described by Dirac fermions because of the linear energy dispersion near the charge neutrality points K and K' at the corner of the Brillouin zone.[15] The relativistic electron dispersion induces particular phenomena, such as the minimum conductivity[3,5,6] and half-integer quantum Hall effects.[3,7,8] An important feature of graphene is its transport properties. Dirac fermions described by the Dirac equation cannot be trapped by a potential barrier because of the Klein paradox.[16] Therefore, localization around the Dirac points ($E = 0$) in graphene is strongly suppressed.[10–14] This behavior is unusual in view of the predictions of scaling theory for conventional two-dimensional disordered electron systems.[17–19]

However, the strong intervalley scattering between the K and K' Dirac cones can lead to localization of electrons in graphene[20–24] when the potential of an impurity changes rapidly in space and large momentum transfer is involved in the scattering processes. Recently, the localized states in disordered graphene near the Dirac points have been observed experimentally.[5] Calculations revealed that different types of disorders could induce different localization behaviors in graphene.[18,19,22,24–26] In the presence of a uniform diagonal disorder in graphene, all states are localized because of the strong intervalley scattering.[18,24] In contrast, for an off-diagonal disorder, the states at the Dirac points are delocalized[24] along the y axis because of the specific chiral symmetry of graphene,[25,27–29] while the states away from the Dirac points remain localized. A further study suggested that in the presence of long-range impurity potentials, states near the Dirac points are also localized,[22] which arises from the increased intervalley scattering caused by the deviation from Dirac dispersion when strong impurities are present. The localization of graphene can be described using single-parameter scaling in all of the above theoretical studies.

Although there are a number of studies on the localization behavior of graphene, it is not clear if this behavior is isotropic. In consideration of the lattice structure, the six-fold rotational symmetry of a honeycomb lattice suggests that the zigzag and armchair axes are not equivalent and the localization of electrons can be affected by the trigonal warping effect. The distinct transport properties of zigzag and armchair nanotubes composed of rolled up graphene strips[10,29] should be related to this point, but the anisotropy of the localization behavior along different axes in graphene has not been studied to date. In addition, when a graphene strip is adhered to a substrate, lattice mismatch is inevitable. The strain induced by the substrate may distort the graphene lattice; dimerization of the A and B sublattices of graphene is the most probable outcome. Such a distortion destroys the six-fold rotational symmetry of the honeycomb lattice and the associated trigonal warping effect, which will also influence the localization behavior of graphene.

*Project supported by the National Basic Research Program of China (Grant No. 2010CB923404), the National Natural Science Foundation of China (Grant No. 11021403), and the National Science Fund for Distinguished Young Scholars of China (Grant No. 10025419).

†Corresponding author. E-mail: wanglmnju@gmail.com

© 2013 Chinese Physical Society and IOP Publishing Ltd

Motivated by the above analyses, we study the localization behavior of both ideal and dimerized graphene structures along different axes by performing a large-scale computation on localization lengths using the standard transfer matrix method. We then analyze the anisotropy of the localization behavior with propagation directions along the y and x axes. Surprisingly, while the states at the Dirac points are delocalized along the y axis with an armchair edge, two-parameter scaled behavior that deviates from conventional scaling theory is found along the x axis with a zigzag edge. Furthermore, the dimerization induced by strain from the substrate suppresses the two-parameter scaled behavior along the x axis, but preserves the delocalized behavior along the y axis. Anisotropy is observed for the localization in graphene with diagonal disorder; it can be tuned by dimerization.

The rest of this paper is organized as follows. In Section 2, we introduce the lattice model and then outline the standard transfer matrix method as well as the finite-size scaling theory. The localization lengths and scaling functions for typical cases are presented in Section 3. Finally, a summary is given in Section 4.

2. Model and method

A tight-binding Hamiltonian in site representation for the π electrons of graphene is

$$H = \sum_i |i\rangle \epsilon_i \langle i| + \sum_{i,j} [t_{ij}|i\rangle\langle j| + \text{h.c.}], \tag{1}$$

where ϵ_i is the on-site energy and t_{ij} is the nearest-neighbor hopping integral. Figure 1 shows the honeycomb lattice of graphene. For an ideal graphene structure, all the on-site energies are the same, as are the nearest-neighbor hopping integrals. The dimerized structure of graphene can be described by identical on-site energies and two different hopping integrals t_1 and t_2 (Fig. 1). We set $t_1 = ct_2$ with $t_2 = 1$ as the energy unit. Thus, the cases with $c > 1$ and $c < 1$ represent two different types of dimerized structures caused by substrate strain, while that with $c = 1$ corresponds to the ideal structure of graphene. For diagonal disorder, ϵ_i is assumed to possess a uniform distribution in the interval $[-W/2, W/2]$, where W is the disorder strength. For off-diagonal disorder, a slight fluctuation of hopping integrals is observed around their average values because of lattice distortion. In this case, t_{ij} is distributed in an interval of $[1-W/2, 1+W/2]*t_1$ or $[1-W/2, 1+W/2]*t_2$, depending on the bond type, where $W(<2)$ is a measure of the deviation from t_1 or t_2.

In the absence of disorder, the electronic band structure for dimerized graphene has the form

$$E_{\pm}(\boldsymbol{k}) = \pm\sqrt{1+4c\cos\left(\frac{3k_x a}{2}\right)\cos\left(\frac{\sqrt{3}k_y a}{2}\right)+4c^2\cos^2\left(\frac{\sqrt{3}k_y a}{2}\right)},$$

where a is the bond length. Consequently, the Dirac points also shift in the momentum space and are given by

$$K = \left(\frac{2\pi}{3a}, +\frac{2\arccos(1/2c)}{\sqrt{3}a}\right)$$

and

$$K' = \left(\frac{2\pi}{3a}, -\frac{2\arccos(1/2c)}{\sqrt{3}a}\right).$$

Obviously, both the positions and shapes of the Dirac cones can be tuned by c.

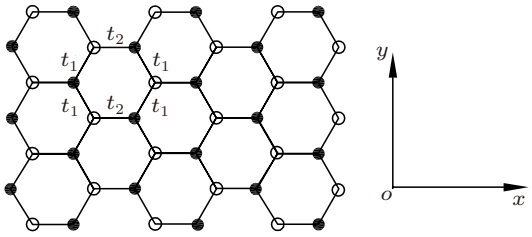


Fig. 1. Diagram of the lattice of dimerized graphene. The filled and empty circles refer to two inequivalent carbon atoms. t_1 and t_2 indicate different bonds because of dimerization. The x and y axes are taken along the armchair and zigzag directions, respectively.

To extract the localization length of graphene, we considered a finite lattice of L rows with M sites in cross section. The relationship between the neighboring rows can be obtained from the tight-binding Schrödinger equations of Hamiltonian Eq. (1)

$$C_{l+1}\psi(l+1) = [EI - H(l)]\psi(l) - C_l\psi(l-1). \tag{2}$$

Here, E is the electronic energy at which the localization property is to be investigated, $H(l)$ and $\psi(l)$ are the Hamiltonian matrix and tight-binding wave function of the l-th row with M components. I is a unit matrix. C_l is the hopping matrix from the $(l-1)$-th row to the l-th row. The exact forms of $H(l)$ and C_l depend on the propagation direction. For a wave function propagating along the y axis, there are two rows in a primitive cell. $H(l)$ and C_l are given by

$$H_l = \begin{pmatrix} \varepsilon_1 & t_2 & & & & \\ t_2 & \varepsilon_2 & & & & \\ & & \varepsilon_3 & t_2 & & \\ & & t_2 & \varepsilon_4 & & \\ & & & & \ddots & \\ & & & & \varepsilon_{M-1} & t_2 \\ & & & & t_2 & \varepsilon_M \end{pmatrix} \tag{3}$$

for odd l rows, and

$$H_l = \begin{pmatrix} \varepsilon_1 & & & & & t_2 \\ & \varepsilon_2 & t_2 & & & \\ & t_2 & \varepsilon_3 & & & \\ & & & \varepsilon_4 & t_2 & \\ & & & t_2 & \varepsilon_5 & \\ & & & & & \ddots \\ t_2 & & & & & \varepsilon_M \end{pmatrix} \tag{4}$$

for even l rows.

$$C_l = \begin{pmatrix} t_1 & & & & & & \\ & t_1 & & & & & \\ & & t_1 & & & & \\ & & & \ddots & & & \\ & & & & t_1 & & \\ & & & & & t_1 & \\ & & & & & & t_1 \end{pmatrix} \tag{5}$$

is the same for both odd and even l.

When the propagation direction is along the x axis, there are four rows in a primitive cell. $H(l)$ has the same form for all the l rows and includes only the diagonal on-site energy. The expression of C_l depends on the exact location in a primitive cell and is given by

$$C_l = \begin{pmatrix} t_1 & t_1 & & & & & \\ & t_1 & t_1 & & & & \\ & & t_1 & t_1 & & & \\ & & & t_1 & t_1 & & \\ & & & & t_1 & t_1 & \\ & & & & & \ddots & \ddots \\ t_1 & & & & & & t_1 \end{pmatrix} \tag{6}$$

for $l = 4n+1$, $n = 0, 1, 2, \ldots$ and

$$C_l = \begin{pmatrix} t_2 & & & & & & \\ & t_2 & & & & & \\ & & t_2 & & & & \\ & & & t_2 & & & \\ & & & & t_2 & & \\ & & & & & \ddots & \\ & & & & & & t_2 \end{pmatrix} \tag{7}$$

for even l. C_l for $l = 4n+3$ is the transpose matrix of Eq. (6).

The recursive relation of Eq. (2) can be extended into transfer matrix form by multiplying it by C_{l+1}^{-1}

$$\begin{aligned} \begin{pmatrix} \psi(l+1) \\ \psi(l) \end{pmatrix} &= \begin{pmatrix} C_{l+1}^{-1}E - C_{l+1}^{-1}H(l) & -C_{l+1}^{-1}C_l \\ I & 0 \end{pmatrix} \begin{pmatrix} \psi(l) \\ \psi(l-1) \end{pmatrix} \\ &= T_l \begin{pmatrix} \psi(l) \\ \psi(l-1) \end{pmatrix}. \end{aligned} \tag{8}$$

Here, T_l is the usual transfer matrix. Thus, for the given initial values of wave functions in the first and second rows, the calculation of the electron propagation along a quasi-one dimensional strip is equivalent to computing the resultant transfer matrix for specified row number L, $G_L = \prod_{l=1}^{L} T_l$. In the thermodynamic limit,

$$G_\infty = \lim_{L\to\infty} (G_L G_L^+)^{1/2L}$$

approaches a limiting matrix according to Oseledec's theorem.[30] Thus, the electronic states and their localization properties are encoded in the eigenvalues and the corresponding eigenfunctions in the limiting matrix. G_L is a symplectic matrix; its eigenvalues appear in pairs with the form $(e^{-\gamma_m(W)}, e^{+\gamma_m(W)})$. $\gamma_m(W)(>0)$s are Lyapunov exponents and their inverse values $1/\gamma_m(W)$ describe the characteristic length scales of their wave functions. The largest length indicates the weakest possible decay of transmission probability along the propagation direction, so the localization length is defined as the smallest value[31,32]

$$\lambda_M(W,E) = \frac{1}{\mathrm{Min}_{m=1,2,\ldots,M}(\gamma_m(W))}. \tag{9}$$

To achieve the required numerical accuracy, a huge number of layers are needed to control the statistical error. To safeguard the information about the smallest eigenvalue, a systematic orthogonalization procedure is carried out during matrix multiplications.[31,32] The accuracy of $\lambda_M(W,E)$ is derived from the variance of the smallest Lyapunov exponent during the course of iteration.

Because the computed data for $\lambda_M(W,E)$ usually cover only a relatively small M, finite-size scaling has to be implemented to extract the localization length for the system with an infinite cross section. This is conducted by treating $\Lambda_M(W,E) = \lambda_M(W,E)/M$ as a proper scaling variable and by fitting all curves with different W into a common scaling function[31,32]

$$\Lambda_M(W,E) = \frac{\lambda_M(W,E)}{M} = f\left(\frac{\xi(W,E)}{M}\right). \tag{10}$$

The scaling parameter $\xi(W,E)$ describes the localization length in the infinite system. It should be emphasized that equation (10) is an ansatz if the scaling theory of localization holds, so it has to be verified by the raw data obtained from the transfer matrix method.

3. Numerical results and discussion

Depending on the value of parameter c, our model describes both an ideal graphene lattice ($c = 1$) and a dimerized one ($c \neq 1$). The dimerized graphene lattice can be stretched along either the x axis ($c > 1$) or the y axis ($c < 1$). Both cases disrupt the six-fold rotational symmetry of the honeycomb lattice. We studied the anisotropic localization behavior of both the ideal and dimerized graphene lattices. In particular, we analyze the interplay between intrinsic and extrinsic effects on the anisotropy of the localization lengths. To guarantee meaningful fitting and obtain reliable scaling parameters, all $\Lambda_M(W,E)$s were calculated with a high accuracy of 1%.

We start our discussion with the ideal graphene lattice. In Fig. 2, the reduced localization length $\Lambda_M(W,E)$ and the scaling function $f(\xi(W,E)/M)$ in the presence of diagonal disorder are plotted for various lateral size M and disorder strength W at the Dirac point. For short-range diagonal disorder, the localization properties were not sensitive to the energy around the Dirac points, so we chose the Dirac point ($E = 0$) as an example. The left and right panels of Fig. 2 show results with the propagation direction along the y and x axes, respectively. Consistent with the single parameter scaling theory and previous studies,[17,18,24] $\Lambda_M(W,E)$s decrease as M increases, which indicates that the electronic states at the Dirac points

are localized for both directions. The reduced localization lengths $\Lambda_M(W,E)$ fall almost perfectly onto a single curve after the scaling parameter $\xi(W,E)$ is introduced for an infinite system. As shown in Fig. 3(a), there is a clear anisotropy in $\xi(W,E=0)$. $\xi(W,E=0)$ along the x axis is larger than that along the y axis. We also calculated the localization lengths away from the Dirac points. The extracted scaling parameters $\xi(W,E)$ are plotted in Fig. 3(b) as functions of energy for $W=6$. Similar to Fig. 3(a), $\xi(W,E)$ along the x axis has a slightly larger value than that along the y axis. The above results clearly suggest that the localization behavior in graphene is intrinsically anisotropic. Although graphene has an isotropic electron dispersion for each Dirac cone K and K', large momentum transfer is involved in this scattering process for short-ranged diagonal disorder, which leads to the strong intervalley scattering between the K and K' Dirac cones. On the other hand, the arrangement of the Dirac cones is a honeycomb lattice in the k space; the y and x axes are along the Γ–K and Γ–M in the Brillouin zone, respectively. Therefore, the propagation along the y and x axes should be distinct during the large momentum transfer, which will induce the anisotropy of the localization behavior.

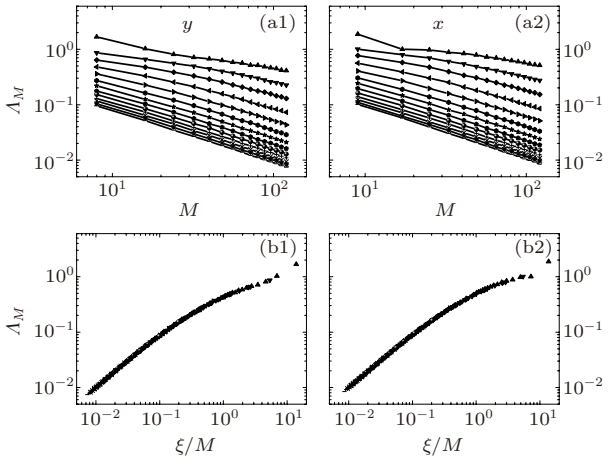


Fig. 2. Reduced localization length and scaling function of ideal graphene at $E=0$ in the presence of a diagonal disorder. The left and right panels refer to the y and x axes, respectively. (a1) and (a2) $\Lambda_M(W,E)$ versus M and W. W has consecutive values of 3–15 from top to bottom; (b1) and (b2) $\Lambda_M(W,E)$ versus $\xi(W,E)/M$.

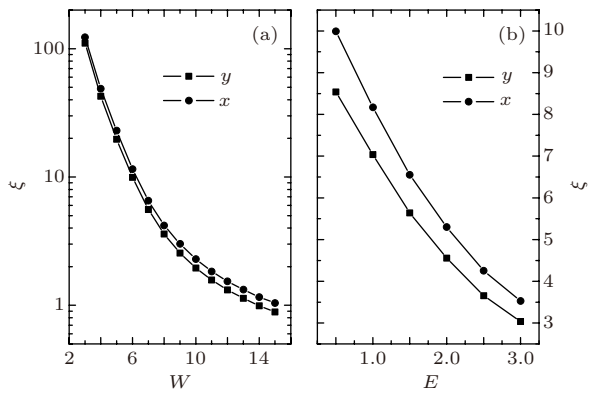


Fig. 3. Scaling parameter $\xi(W,E)$ of ideal graphene in the presence of a diagonal disorder. (a) $\xi(W,E)$ versus W at $E=0$; (b) $\xi(W,E)$ versus E at $W=6$.

In the presence of an off-diagonal disorder, the localization property is very sensitive to the energy around the Dirac points because intervalley scattering is weak and intravalley scattering is determined by the phase space available near the Dirac points. The reduced localization lengths $\Lambda_M(W,E)$ shown in Figs. 4(a1) and 4(a2) for the energy $E=0.0001$ close to the Dirac points along the y and x axes, respectively, were used to determine the two-dimensional localization properties of graphene. In contrast to the diagonal disorder, an off-diagonal disorder should not break the chiral symmetry at the Dirac points, so delocalized states are expected.[10,24] This is indeed the case when the chosen propagation direction is along the y axis with an armchair edge. As shown in Fig. 4(a1), the calculated localization length is independent of M for all the disorder strengths and $\xi(W,E)$ tends to infinity, which indicates the delocalized state. A completely different scenario occurs when the localization length is computed along the x axis. Figure 4(a2) reveals that $\Lambda_M(W,E)$s are naturally divided into two classes with lateral size $M=3l$ and $M=3l\pm1$ (l is an integer) that show two-parameter scaling. For the class $M=3l$, the localization length is essentially the same as that along the y axis. In contrast, for the class $M=3l\pm1$, the localization length is independent of both the lateral size M and the disorder strength W. Previous studies showed that either strong coupling effects[33] or magnetic fields[34] plus disorder can induce the breakdown of single-parameter scaling. However, our study indicates that this breakdown occurs around the Dirac point of graphene in the presence of an off-diagonal disorder. The anisotropy of the localization behavior near the Dirac points has some resemblance to that of carbon nanotubes predicted by the simple zone-folding scheme. It is well known that undoped armchair nanotubes and class $M=3l$ zigzag nanotubes are metallic, whereas classes $M=3l\pm1$ zigzag nanotubes are semiconducting.[29] The situation for a graphene strip with cross section M is similar under the lateral periodic boundary conditions. For metallic graphene strips, $\Lambda_M(W,E)$ is independent of M and decreases slowly with increasing W, while for semiconducting graphene strips, $\Lambda_M(W,E)$ is independent of both M and W. This suggests that the localization behavior near the Dirac points depends on the phase space accessible for intravalley scattering and the availability of electronic modes at this particular energy. The localization behavior becomes normal when the energy is away from the Dirac point. As shown in Figs. 4(b1) and 4(b2) for $E=0.01$, the localized behavior recovers when $W\geq1.5$. In addition, the two-parameter scaling behavior along the x axis weakens when $W>1.5$. The extracted scaling parameter $\xi(W,E)$ is plotted as functions of energy E in Fig. 5. Excluding the vicinity of the Dirac points, the states at other energies are all localized, even for a small disorder strength. The anisotropic localization of electrons in graphene is clearly demonstrated for all energies.

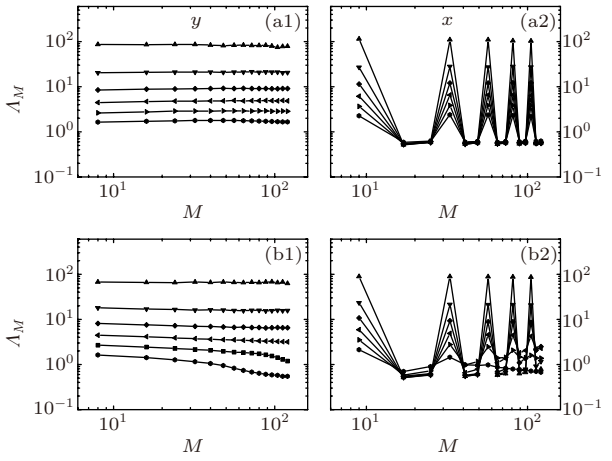


Fig. 4. Reduced localization length of ideal graphene in the presence of an off-diagonal disorder. $\Lambda_M(W,E)$ versus M and W along the y axis for $E = 0.0001$ (a1) and $E = 0.01$ (b1); $\Lambda_M(W,E)$ versus M and W along the x axis for $E = 0.0001$ (a2) and $E = 0.01$ (b2). From top to bottom $W = 0.3, 0.6, 0.9, 1.2, 1.5, 1.8$.

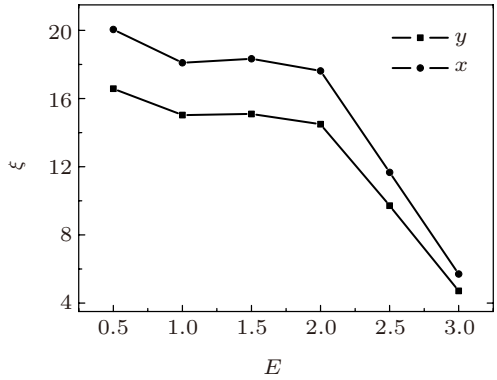


Fig. 5. Scaling parameter $\xi(W,E)$ versus energy E of ideal graphene in the presence of an off-diagonal disorder. $W = 1.8$.

We now consider dimerized graphene. When the strain induced by a substrate tends to elongate the graphene lattice along the y axis and $t_1 < t_2$, electron propagation along the y axis is suppressed with respect to that along the x axis. Here, we used $t_1 = 0.8t_2$ and the unperturbed band spanning from -2.6 to 2.6. The extracted $\xi(W,E)$s obtained under a diagonal disorder are plotted as a function of disorder W at the Dirac points in Fig. 6(a) and as a function of energy E at $W = 6$ in Fig. 6(b). Figure 6 indicates that the electron states along the x axis are generally less localized than those along the y axis. As a result, the anisotropy is enhanced compared with that of ideal graphene, as shown in Fig. 3.

Although dimerization of the graphene destroys the sixfold rotational symmetry of the honeycomb lattice and causes the Dirac cones to change from an isotropic to anisotropic shape, chiral symmetry remains in the vicinity of the Dirac points for an off-diagonal disorder. One could expect that dimerization does not fundamentally change the localization behavior around the Dirac points. This proved to be true only along the y axis. Λ_M in Fig. 7(a1) looks like Fig. 4(a1); the wave function shows a typical delocalized feature. Qualitatively, the weaker hopping along the y axis reduces the localization length along it. However, the localization behavior along the x axis changes dramatically, as can be seen in Fig. 7(a2). Because the shift of the Dirac points in the momentum space invalidates the classification of graphene strips into $M = 3l$ and $M = 3l \pm 1$, the difference in the scaling behavior between the two classes is completely suppressed by the dimerization. The localization lengths fluctuate with the lateral size M for various disorder strengths and no tendency to converge is observed. This reflects the sensitivity of the electron modes available at the Dirac points when the sixfold rotational symmetry is broken. Similar to ideal graphene, such behavior ceases when the energy moves away from the Dirac point and enough phase space for intravalley scattering becomes available. As shown in Fig. 7(b1), the usual localization behavior is already recovered at $E = 0.01$ for moderate disorder strength.

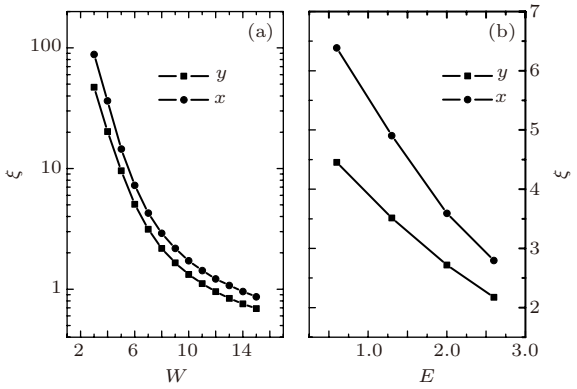


Fig. 6. Scaling parameter $\xi(W,E)$ of dimerized graphene ($t_1 = 0.8t_2$) in the presence of a diagonal disorder. (a) $\xi(W,E)$ versus W at $E = 0$; (b) $\xi(W,E)$ versus E at $W = 6$.

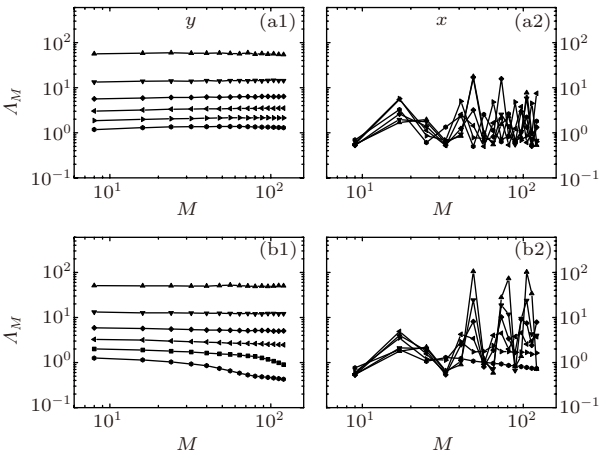


Fig. 7. Reduced localization length of dimerized graphene ($t_1 = 0.8t_2$) in the presence of an off-diagonal disorder. $\Lambda_M(W,E)$ versus M and W along the y axis for $E = 0.0001$ (a1) and $E = 0.01$ (b1); $\Lambda_M(W,E)$ versus M and W along the x axis for $E = 0.0001$ (a2) and $E = 0.01$ (b2). From top to bottom $W = 0.3, 0.6, 0.9, 1.2, 1.5, 1.8$.

When the strain induced by the substrate tends to elongate graphene along its x axis, the opposite scenario with $t_1 > t_2$ appears. Specifically, we considered $t_1 = 1.2t_2$ and the unperturbed band spanning from -3.4 to 3.4. Similar to previous cases with diagonal disorder, the states are all localized and can be fitted nicely into a common scaling curve. The scaling

parameter $\xi(W,E)$ is plotted at the Dirac points and other energies in Fig. 8. In this case, some compensation takes place between the intrinsic effect of graphene and the extrinsic effect of dimerization; the localization length exhibits perfect isotropic behavior in the presence of a diagonal disorder. For an off-diagonal disorder, the results along the y and x axes are quite similar. As shown in Figs. 9(a1) and 9(b1), larger hopping along the y axis tends to increase the localization length, as expected physically. For the localization behavior along the x axis (Figs. 9(a2) and 9(b2)), the situation is the same as the dimerized case discussed above.

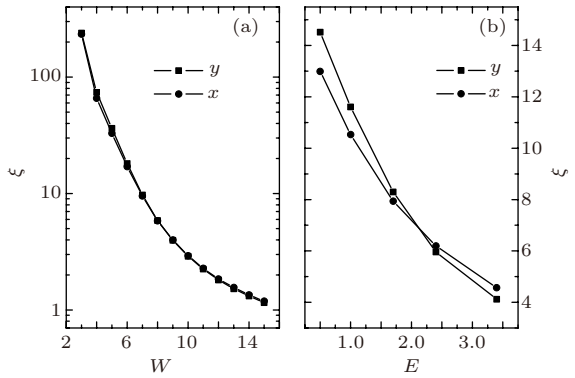


Fig. 8. Scaling parameter $\xi(W,E)$ of dimerized graphene ($t_1 = 1.2t_2$) in the presence of a diagonal disorder. (a) $\xi(W,E)$ versus W at $E = 0$; (b) $\xi(W,E)$ versus E at $W = 6$.

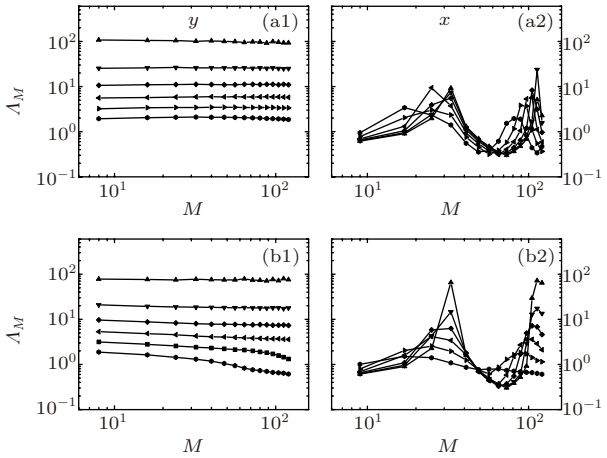


Fig. 9. Reduced localization length of dimerized graphene ($t_1 = 1.2t_2$) in the presence of an off-diagonal disorder. $\Lambda_M(W,E)$ versus M and W along the y axis for $E = 0.0001$ (a1) and $E = 0.01$ (b1); $\Lambda_M(W,E)$ versus M and W along the x axis for $E = 0.0001$ (a2) and $E = 0.01$ (b2). From top to bottom $W = 0.3, 0.6, 0.9, 1.2, 1.5, 1.8$.

4. Conclusion

In conclusion, the reduced localization lengths, scaling function and scaling parameter $\xi(W,E)$ were calculated for graphene and dimerized graphene along different propagation directions using the transfer matrix method and finite-size scaling. In the presence of a diagonal disorder, the localization lengths can all be fitted into a common scaling curve, validating the single parameter scaling theory. However, for an off-diagonal disorder, while the states at the Dirac points were delocalized along the y axis with armchair edges, two-parameter scaled behavior appeared along the x axis with zigzag edges. Except for the Dirac points, the localization lengths of graphene with an off-diagonal disorder also satisfied the single parameter scaling theory. Our results demonstrate that the localization behavior of ideal graphene was strongly anisotropic in the presence of either a diagonal or an off-diagonal disorder. The dimerization of graphene may either strengthen or weaken this anisotropic localization behavior, which depends on the specific structural distortion of graphene.

References

[1] Novoselov K S, Geim A K, Morozov S V, Jiang D, Zhang Y, Dubonos S V, Grigorieva I V and Firsov A A 2004 *Science* **306** 666

[2] Novoselov K S, Jiang D, Schedin F, Booth T J, Khotkevich V V, Morozov S V and Geim A K 2005 *Proc. Natl. Acad. Sci. USA* **102** 10451

[3] Novoselov K S, Geim A K, Morozov S V, Jiang D, Katsnelson M I, Grigorieva I V, Dubonos S V and Firsov A A 2005 *Nature* **438** 197

[4] Castro Neto A H, Guinea F, Peres N M R, Novoselov K S and Geim A K 2009 *Rev. Mod. Phys.* **81** 109

[5] Adam S, Cho S, Fuhrer M S and Das Sarma S 2008 *Phys. Rev. Lett.* **101** 046404

[6] Huard B, Sulpizio J A, Stander N, Todd K, Yang B and Goldhaber-Gordon D 2007 *Phys. Rev. Lett.* **98** 236803

[7] Zhang Y B, Tan Y W, Stormer H L and Kim P 2005 *Nature* **438** 201

[8] Zhang Y B, Jiang Z, Small J P, Purewal M S, Tan Y W, Fazlollahi M, Chudow J D, Jaszczak J A, Stormer H L and Kim P 2006 *Phys. Rev. Lett.* **96** 136806

[9] Sun L F, Dong L M, Wu Z F and Fang C 2013 *Chin. Phys. B* **22** 077201

[10] Ando T and Nakanishi T 1998 *J. Phys. Soc. Jpn.* **67** 1704

[11] Bardarson J H, Tworzydlo J, Brouwer P W and Beenakker C W J 2007 *Phys. Rev. Lett.* **99** 106801

[12] Nomura K, Koshino M and Ryu S 2007 *Phys. Rev. Lett.* **99** 146806

[13] Altland A 2006 *Phys. Rev. Lett.* **97** 236802

[14] Ziegler K 1998 *Phys. Rev. Lett.* **80** 3113

[15] Wallace P R 1947 *Phys. Rev.* **71** 622

[16] Katsnelson M I, Novoselov K S and Geim A K 2006 *Nat. Phys.* **2** 620

[17] Abrahams E, Anderson P W, Licciardello D C and Ramakrishnan T V 1979 *Phys. Rev. Lett.* **42** 673

[18] Schreiber M and Ottomeier M 1992 *J. Phys.: Condens. Matter* **4** 1959

[19] Ziman T A L 1982 *Phys. Rev. B* **26** 7066

[20] Morpurgo A F and Guinea F 2006 *Phys. Rev. Lett.* **97** 196804

[21] Pereira V M, Guinea F, Lopes dos Santos J M B, Peres N M R and Castro Neto A H 2006 *Phys. Rev. Lett.* **96** 036801

[22] Zhang Y Y, Hu J P, Bernevig B A, Wang X R, Xie X C and Liu W M 2009 *Phys. Rev. Lett.* **102** 106401

[23] Amini M, Jafari S A and Shahbazi F 2009 *Europhys. Lett.* **87** 37002

[24] Xiong S J and Xiong Y 2007 *Phys. Rev. B* **76** 214204

[25] Mucciolo E R and Lewenkopf C H 2010 *J. Phys.: Condens. Matter* **22** 273201

[26] Fischer A M, Römer R A and Dzyubenko A B 2011 *Phys. Rev. B* **84** 165431

[27] Gade R and Wegner F 1991 *Nucl. Phys. B* **360** 213

[28] Fabrizio M and Castellani C 2000 *Nucl. Phys. B* **583** 542

[29] Charlier J C, Blase X and Roche S 2007 *Rev. Mod. Phys.* **79** 677

[30] Oseledec V I 1968 *Trans. Moscow Math. Soc.* **19** 197

[31] MacKinnon A and Kramer B 1983 *Z. Phys. B* **53** 1

[32] Kramer B and MacKinnon A 1993 *Rep. Prog. Phys.* **56** 1469

[33] Campo V L, Capelle K, Quintanilla J and Hooley C 2007 *Phys. Rev. Lett.* **99** 240403

[34] Onoda M and Nagaosa N 2003 *Phys. Rev. Lett.* **90** 206601